

1 **A WD40 repeat-like protein pathway connects F-BOX STRESS INDUCED (FBS) proteins**
2 **to the NIGT1.1 transcriptional repressor in *Arabidopsis***

5 **Edgar Sepulveda-Garcia^{1,2}, Elena C Fulton^{3†}, Emily V Parlan^{3†}, Ashley A Brauning³, Lily**
6 **E O'Connor³, Anneke A Fleming³, Amy J Replogle³, Mario Rocha-Sosa², Joshua M**
7 **Gendron⁴, Bryan Thines^{3*}**

10 1 Instituto de Biotecnología, Universidad del Papaloapan, Tuxtepec 68301, Mexico

11 2 Departamento de Biología Molecular de Plantas, Instituto de Biotecnología, Universidad
12 Nacional Autónoma de México, Cuernavaca, Mor, 62250, Mexico

15 3 Biology Department, University of Puget Sound, Tacoma, WA 98416, USA

17 4 Department of Molecular, Cellular, and Developmental Biology, Yale University, New
18 Haven, Connecticut 06511, USA

20 [†] These authors have contributed equally to this work

23 *** Correspondence:**

24 Bryan Thines

25 bthines@pugetsound.edu

28 **Keywords: F-box protein, SCF complex, stress response, transcription regulation, WD40**
29 **repeat-like protein**

47 **ABSTRACT**

48

49 SCF-type E3 ubiquitin ligases use F-box (FBX) proteins as interchangeable substrate adaptors to
50 recruit protein targets for ubiquitylation. FBX proteins almost universally have structure with
51 two domains. A conserved N-terminal F-box domain interacts with a SKP protein and connects
52 the FBX protein to the core SCF complex, while a C-terminal domain interacts with the protein
53 target and facilitates recruitment. The F-BOX STRESS INDUCED (FBS) subfamily of four
54 plant FBX proteins has atypical domain structure, however, with a centrally located F-box
55 domain and additional conserved regions at both the N- and C-termini. FBS proteins have been
56 linked to environmental stress networks, but no ubiquitylation target(s) or exact biological
57 function has been established for this subfamily. We have identified two WD40 repeat-like
58 proteins in *Arabidopsis* that are highly conserved in plants and interact with FBS proteins, which
59 we have named FBS INTERACTING PROTEINS (FBIPs). FBIPs interact exclusively with the
60 N-terminus of FBS proteins, and this interaction occurs in the nucleus. FBS1 destabilizes FBIP1,
61 consistent with FBIPs being ubiquitylation targets of SCF^{FBS} complexes. Furthermore, we found
62 that FBIP1 interacts with NIGT1.1, a GARP-type transcriptional repressor that regulates nitrate
63 and phosphate starvation signaling and responses. Collectively, these interactions between FBS,
64 FBIP, and NIGT1.1 proteins delineate a previously unrecognized SCF-connected transcription
65 regulation module that works in the context of phosphate and nitrate starvation, and possibly
66 other environmental stresses. Importantly, this work also identified two uncharacterized WD40
67 repeat-like proteins as new tools with which to probe how an atypical SCF complex, SCF^{FBS},
68 functions via FBX protein N-terminal interaction events.

69

70

71

72

73

74

75

76

77

78

79

80

81

82

83

84

85

86

87

88

89

90

91

92

93 **INTRODUCTION**

94

95 Essential plant processes, ranging from growth and development to stress responses, are
96 controlled at the molecular level through selective protein degradation by the ubiquitin 26S
97 proteasome system (UPS). Protein targets destined for removal are ubiquitylation substrates for
98 E3 ubiquitin ligases, where one prevalent E3 ligase subtype is the SKP1-Cullin-F-box (SCF)
99 complex (Hua and Vierstra, 2011). SCF complexes use an interchangeable F-box (FBX) protein
100 subunit as a substrate adaptor to specifically interact with unique protein targets (Gagne et al.,
101 2002; Sheard et al., 2010; Calderon Villalobos et al., 2012). FBX proteins almost universally
102 have structure with two domains: an N-terminal F-box domain facilitates interaction with a SKP
103 protein and the core SCF complex and a C-terminal domain interacts specifically with the
104 target(s) (Gagne et al., 2002). This two-domain structure directly bridges core UPS components
105 to precise protein targets under specific situations, and it places FBX proteins at a dynamic
106 interface that regulates diverse cellular output pathways.

107

108 A very small number of FBX proteins across eukaryotes, however, deviate from this typical two-
109 domain protein structure. Many of these atypical FBX proteins have a centrally located F-box
110 domain, a C-terminal target interaction domain, and an additional protein interaction domain at
111 the N-terminus (Jin, 2004; Wang et al., 2014; Lee et al., 2018). In humans, N-terminal domains
112 can control subcellular localization (Matsumoto et al., 2011), bind to an accessory protein that
113 assists with C-terminal targeting events (Spruck et al., 2001), or mediate regulatory interactions
114 with other proteins (Jin, 2004; Kirk et al., 2008; Nelson et al., 2013). The only plant FBX
115 proteins with established N-terminal interaction dynamics belong to the ZEITLUPE (ZTL),
116 FLAVIN-BINDING KELCH REPEAT F-BOX1 (FKF1), and LOV KELCH PROTEIN2 (LKP2)
117 subfamily, which regulates the circadian clock and flowering time (Yasuhara, 2004; Kim et al.,
118 2007; Sawa et al., 2007; Zoltowski and Imaizumi, 2014; Lee et al., 2018). In addition to a central
119 F-box domain, the ZTL/FKF1/LKP2 subfamily has an N-terminal blue-light sensing LOV
120 domain and C-terminal kelch repeats (Zoltowski and Imaizumi, 2014), which are both used to
121 recruit distinct ubiquitylation substrates (Más et al., 2003; Yasuhara, 2004; Song et al., 2014; Lee
122 et al., 2018). The N-terminal LOV domain has additional roles that regulate FBX function
123 through interaction with GIGANTEA (GI), which controls subcellular localization and protein
124 stability (Kim et al., 2007; Sawa et al., 2007). Thus, across kingdoms, atypical FBX proteins
125 with an N-terminal protein interaction domain, in addition to a C-terminal targeting domain,
126 achieve expanded function by having further regulatory capacity and/or coordinating multiple
127 cellular outputs through a dual targeting structure.

128

129 F-BOX STRESS INDUCED (FBS) proteins are a far less understood subfamily of four plant
130 FBX proteins with atypical structure (Maldonado-Calderon et al., 2012; Sepulveda-Garcia and
131 Rocha-Sosa, 2012; Gonzalez et al., 2017). FBS1 is the founding member of this FBX subfamily
132 and is recognized for its broad biotic and abiotic stress responsive gene induction profiles
133 (Maldonado-Calderon et al., 2012; Gonzalez et al., 2017). In FBS1, a centrally located F-box
134 domain is flanked by two conserved regions present at the N- and C-termini, which do not match
135 any known protein interaction domains or motifs (Maldonado-Calderon et al., 2012). FBS1
136 interacts with *Arabidopsis* SKP1 (ASK1) and can autoubiquitylate (Maldonado-Calderon et al.,
137 2012; Sepulveda-Garcia and Rocha-Sosa, 2012), suggesting that it forms a functional SCF-type
138 E3 ligase *in vivo*. At least five of thirteen *Arabidopsis* 14-3-3 regulatory proteins bind to FBS1

139 (Sepulveda-Garcia and Rocha-Sosa, 2012). However, because this interaction requires both the
140 N-terminal region and the F-box domain of FBS1 (Sepulveda-Garcia and Rocha-Sosa, 2012),
141 and ubiquitylation presumably requires an unhindered F-box domain to interact with the SKP
142 subunit of the SCF complex (Hua and Vierstra, 2011), 14-3-3s are unlikely ubiquitylation
143 targets. Furthermore, an inducible *FBS1* gene construct had no discernable effect on FBS1
144 interactor 14-3-3 λ protein abundance (Sepulveda-Garcia and Rocha-Sosa, 2012). Importantly
145 though, all five FBS1-interacting 14-3-3 proteins are negative regulators in *Arabidopsis*
146 responses to cold and/or salt stress (Catala et al., 2014; van Kleeff et al., 2014; Zhou et al.,
147 2014), which demonstrates another noteworthy cellular link between FBS1 and environmental
148 stress response networks beyond the broad stress-inducible transcriptional regulation of *FBS1*.
149

150 More complete understanding of FBS protein function in plants has been stymied by two primary
151 limitations. First, not knowing selective targeting relationship(s) between SCF^{FBS} complexes and
152 their substrates has left FBS action on cellular output pathways completely enigmatic. Second,
153 functional redundancy within this family has likely thwarted past efforts seeking to establish a
154 biological function based on phenotype of *Arabidopsis fbs1* plants (Maldonado-Calderon et al.,
155 2012; Gonzalez et al., 2017), but no evidence for redundancy exists to confirm this as an
156 experimental barrier. Here, we identify two highly conserved WD40 repeat-like proteins that
157 interact with multiple FBS family members in *Arabidopsis*, which we have named FBS
158 INTERACTING PROTEINs (FBIPs). Interactions between all four FBS subfamily members and
159 FBIP proteins occur in the nucleus, and interactions occur exclusively via the N-terminal domain
160 of FBS proteins. FBIP1 also interacts in the nucleus with NIGT1.1, a DNA-binding GARP
161 transcriptional repressor and key regulator of plant nitrate and phosphate signaling and starvation
162 responses (Kiba et al., 2018; Maeda et al., 2018; Ueda et al., 2020a, 2020b). This FBS-FBIP-
163 NIGT1.1 network of newly identified protein interactions strongly suggests the possibility that
164 FBS family proteins use N-terminal interaction events to regulate stress genes and, in particular,
165 genes involved in nitrate and phosphate starvation responses and signaling.
166
167

168 METHODS

169 Bioinformatics

170 Gene and protein sequences were obtained from The *Arabidopsis* Information Resource
171 (www.arabidopsis.org). Protein sequences were aligned using T-COFFEE
172 (www.ebi.ac.uk/Tools/msa/tcoffee) accessed through the European Bioinformatics Institute
173 (EBI) website (www.ebi.ac.uk). WD40 repeat-like sequences were identified in FBIP1 and
174 FBIP2 using the WD40-repeat protein Structures Predictor data base version 2.0 (WDSPdb 2.0;
175 www.wdspdb.com) (Ma et al., 2019). Basic Local Alignment Search Tool (BLAST) and
176 Position-Specific Iterative (PSI)-BLAST were accessed through the National Center for
177 Biotechnology Information (NCBI) website (www.ncbi.nlm.nih.gov) and used to search the
178 RefSeq database. Candidate protein interactors were identified by searching the SUBA4 database
179 (www.suba.live) (Hooper et al., 2017).
180

181 Gateway cloning

182
183
184

185 Gene-specific primers (Supplementary Table S1) were used with PCR to amplify coding
186 sequences from pooled *Arabidopsis thaliana* (accession Col-0) cDNA. Amplicons were inserted
187 into pENTR/D-TOPO vector (ThermoFisher Scientific) according to the manufacturer's
188 protocols. Genes were then transferred with LR Clonase II enzyme mix (ThermoFisher
189 Scientific) into pCL112 or pCL113 (Zhu et al., 2008a) destination vectors for BiFC experiments,
190 and into pGBKT7-GW (Addgene plasmid #61703) or pGADT7-GW (Addgene plasmid #61702)
191 destination vectors for yeast two-hybrid experiments. Alternatively (Figure 3B), *FBS1* and
192 *FBIP1* sequences were cloned into pBI770/pBI771 and tested for interaction, as done previously
193 (Sepulveda-Garcia and Rocha-Sosa, 2012). Primers used to create *FBS1* truncation constructs are
194 indicated in Supplementary Table S1.

195
196 **Yeast two-hybrid assays**

197
198 *Saccharomyces cerevisiae* cells were grown, transformed, mated, and selected for by standard
199 yeast protocols. Bait constructs (GAL4 DNA-binding domain, DBD) were transformed into Y2H
200 Gold and prey constructs (GAL4 activation domain, AD) into Y187 strains by LiAc method
201 (Takara Bio USA). Haploid strains were mated to produce diploid strains to test for interactions.
202 Diploid strains were grown for 24 hours at 30 °C in liquid synthetic defined (SD) medium minus
203 Trp/Leu (-TL) medium with shaking. Cells were then washed in sterile water, cell concentrations
204 were adjusted to OD₆₀₀ = 10⁰, 10⁻¹, 10⁻², 10⁻³, and 10 µL was spotted on SD -TL (control), SD
205 minus Trp/Leu/His (-TLH), and SD minus Trp/Leu/His (-TLHA) selective plates. Plates were
206 incubated for two days at 30 °C and then scanned to produce images.

207
208 **Bimolecular fluorescence complementation (BiFC)**

209
210 Recombinant plasmids were transformed into *Agrobacterium tumefaciens* strain GV3101
211 (pMP90) by electroporation and selected under appropriate antibiotics. *A. tumefaciens* seed
212 cultures were grown in LB with appropriate antibiotic selection for two days with shaking at 30
213 °C and then used to inoculate 50 mL LB containing appropriate antibiotics plus 10 µM
214 acetosyringone and grown for an additional 24 hours. Cells were pelleted and resuspended in
215 infiltration medium (10 mM MES, 10 mM MgCl₂, 100 µM acetosyringone) and incubated for
216 five hours with rocking at room temperature. Cells were pelleted a second time, resuspended in
217 infiltration medium and appropriate nYFP/cYFP, H2B-RFP constructs were combined at a final
218 OD₆₀₀ of 1.0 for each test/control construct with suppressor strains (p19, γβ, PtoHA, HcPro) at a
219 final OD₆₀₀ of 0.5. *Nicotiana benthamia* leaves from four week-old plants were infiltrated by
220 syringe with the *A. tumefaciens* mixes. The underside of whole leaf mounts was visualized using
221 laser-scanning confocal microscopy three days after infiltration with a Nikon D-Eclipse C1
222 Confocal laser scanning microscope (Nikon Instruments) with either: 1) excitation at 488 nm
223 with an emission band pass filter of 515/30, or 2) excitation at 561 nm with an emission band
224 pass filter of 650 LP.

225
226 **Co-infiltration**

227
228 *FBS1*, *FBIP1*, and 14-3-3λ were cloned into pGWB17 (4X myc tag), pGWB14 (3X HA tag), or
229 pGWB12 (VSVG tag) vectors (Nakagawa et al., 2007), respectively, using a Gateway strategy as
230 above. Recombinant plasmids were transformed by electroporation into *A. tumefaciens* strain

231 C58C1Rif/pGV2260. *A. tumefaciens* was grown to stationary phase in LB medium containing
232 appropriate antibiotics plus 50 µg/ml acetosyringone. Bacteria were pelleted and washed with 10
233 mM MgCl₂, and then resuspended in 10 mM MgCl₂ and 150 µg/ml acetosyringone. Cell
234 densities were adjusted to OD₆₀₀ of 0.5. After 3 h of incubation, *A. tumefaciens* strains containing
235 each construct were adjusted to varying concentrations and mixed with the same volume of an *A.*
236 *tumefaciens* strain containing the viral suppressor p19, treated in the same way, but adjusted to
237 OD₆₀₀ of 1.0. The abaxial side of leaves from 3-4 week-old *N. benthamiana* were infiltrated with
238 this bacterial suspension. After 3 days, leaf material was collected and immediately frozen in
239 liquid N₂ for protein extraction.

240

241 Protein extraction and Western blotting

242

243 Approximately 100 µg of frozen tissue was homogenized in 200 µl of 1X Laemmli loading
244 buffer plus 4 M urea, boiled 5 minutes and centrifuged at 10,000 x g for five minutes. 10 µl of
245 the supernatant were loaded onto 8%, 10%, or 15% polyacrylamide gels and subjected to SDS-
246 PAGE using standard protocols. Separated proteins were blotted onto a Hybond-P+ membrane
247 (Amersham Pharmacia Biotech) using standard protocols, and then membranes were probed with
248 anti-c-Myc, anti-HA antibody, or anti-VSVG antibodies (all from Sigma). Blots were developed
249 using an alkaline phosphatase kit (BCIP/NBT kit; Invitrogen).

250

251 AGI numbers

252

253 FBS1 (At1g61340), FBS2 (At4g21510), FBS3 (At4g05010), FBS4 (At4g35930), FBIP1
254 (At3g54190), FBIP2 (At2g38630), NIGT1.1 (At1g25550)

255

256

257 RESULTS

258

259 FBS protein interaction with ASK1

260 FBS1 is the founding protein of a four-member FBX protein subfamily (FBS1 – FBS4). FBS2 –
261 FBS4, like FBS1, share non-canonical structure with a centrally located F-box domain and
262 conserved regions at their N- and C- termini (Figure 1A). The conserved region at FBS N-
263 termini spans approximately 20 residues, while the conserved region at the C-terminus
264 encompasses about 35 (Figure 1A). FBS1 interacts with ASK1 and autoubiquitylates, indicating
265 FBS1 likely participates in functional SCF complexes (Maldonado-Calderon et al., 2012;
266 Sepulveda-Garcia and Rocha-Sosa, 2012). However, the ability of other FBS family members to
267 interact with ASK proteins remains unknown, as does the possibility of functional redundancy
268 among family members. To interrogate this possibility, all four FBS family members were tested
269 as bait constructs (DBD, GAL4 DNA-binding domain) for interaction with ASK1 as prey (AD,
270 GAL4 activation domain) under less stringent (-TLH) and more stringent (-TLHA) nutritional
271 selection. Interactions were apparent between all four FBS family members on -TLH, although
272 only very minimal growth was observed for FBS2 (Figure 1B). Only interactions between FBS1
273 and FBS4 with ASK1 were apparent under most stringent selection (-TLHA) (Figure 1B). Since
274 Arabidopsis has 21 ASK proteins, it is possible the FBS proteins showing minimal partnering
275 with ASK1 instead interact more strongly with other untested ASKs (Kuroda et al., 2012). These

276 interactions show, however, that all FBS2 – FBS4 are viable candidates for functional SCF
277 complex substrate adapters, like FBS1.

278

279 **Identification of a new FBS1 interactor**

280

281 In addition to ASK1, the only known FBS1 interacting proteins are 14-3-3 proteins (Sepulveda-
282 Garcia and Rocha-Sosa, 2012). However, because interaction dynamics are not consistent with
283 ubiquitylation of 14-3-3 proteins by SCF^{FBS1} (Sepulveda-Garcia and Rocha-Sosa, 2012), we
284 sought additional FBS1 interactors as candidate targets that could connect FBS proteins to
285 biological processes. Two additional related proteins were identified as partners for FBS1, which
286 we have named FBS INTERACTING PROTEINs (FBIPs). FBIP1 (At3g54190) was identified in
287 the same yeast two-hybrid screen that found 14-3-3 proteins as FBS1 interactors (Sepulveda-
288 Garcia and Rocha-Sosa, 2012). FBIP1 is also listed as an FBS1 interactor by the SUBA4
289 database (www.suba.live) from previous high-throughput protein-protein interaction (PPI)
290 screening (Arabidopsis Interactome Mapping Consortium et al., 2011; Hooper et al., 2017).
291 FBIP1 is 467 residues in length and is a member of the transducin / WD40 repeat-like
292 superfamily of proteins. WD40 repeats typically form a β -propeller domain that acts as a scaffold
293 in mediating protein-protein or protein-DNA interactions (Jain and Pandey, 2018). Seven
294 putative WD40 repeat-like sequences were predicted in FBIP1 by the WD40-repeat protein
295 Structures Predictor database version 2.0 (WDSPdb 2.0) (Ma et al., 2019), although these
296 predictions fall into the low confidence category (Figure 2). A second FBIP protein (At2g38630)
297 was identified in the Arabidopsis genome by BLAST search, which we have named FBIP2.
298 Protein sequence identity and similarity between FBIP1 and FBIP2 are just over 91% and 96%,
299 respectively (Figure 2).

300

301 We gained no additional insight about FBIP function using various bioinformatics resources.
302 Other than putative WD repeat-like sequences, no sequence features were identified using
303 various domain or motif prediction programs. BLAST and PSI-BLAST searches with FBIP1 and
304 FBIP2 sequences failed to identify additional significant hits in Arabidopsis. We did, however,
305 find very highly conserved FBIP sequences throughout the plant kingdom, including in
306 bryophytes (the top BLAST hit in *Physcomitrella patens* is about 77% identical and 85% similar
307 to *Arabidopsis* FBIP1). By investigating AtGenExpress ATH1 array data sets (Schmid et al.,
308 2005; Kilian et al., 2007; Goda et al., 2008), we found that *FBIP1* is constitutively expressed in
309 most tissues and organs of *Arabidopsis*, and throughout its life cycle, but we found no conditions
310 where *FBIP1* is more highly expressed compared to other conditions. *FBIP2* is not represented
311 on the ATH1 array.

312

313 **FBS interactions with FBIPs**

314

315 We confirmed that full-length FBS1 and FBIP1 interact by yeast two-hybrid analysis. Interaction
316 between FBS1 and FBIP1 elicited growth in yeast strains on both less stringent (-TLH) and more
317 stringent (-TLHA) nutritional selection, and FBS1 yielded growth with FBIP2 on -TLH (Figure
318 3A). Family-wide interactions between each FBS protein and the two FBIP proteins were also
319 assessed (Figure S1). Growth was also observed for FBS3 and FBIP1, but not with FBS2 or
320 FBS4. No additional interactions were observed with FBIP2. Collectively, yeast two-hybrid
321 results suggest that FBS1 and FBIP1 might be the primary FBS-FBIP protein interaction pair, or

322 possibly bind with strongest affinity, but that some other family-wide interactions might be
323 possible.

324
325 FBS proteins have two regions of unknown function outside of the F-box domain and,
326 presumably, at least one of these interacts with a target. In order to determine which parts of
327 FBS1 are important for FBIP1 interaction, we created truncated versions of FBS1 with the N-
328 terminal (NT), F-box, or C-terminal (CT) regions removed in different combinations and tested
329 under stringent (-TLHA) selection (Figure 3B). Removing the N-terminal region (Δ NT-FBS1₁₈₁₋₁₈₅)
330 abolished the ability of FBS1 to interact with FBIP1, while removal of the F-box domain
331 (Δ F-FBS1₁₈₄₋₁₃₅) or C-terminal region (Δ CT-FBS1₁₁₋₁₂₈) did not. The FBS1 N-terminal region
332 (NT-FBS1₁₋₈₀) in combination with full-length FBIP1 yielded growth on -TLHA, indicating that
333 the FBS1 N-terminal domain alone is sufficient to mediate this interaction.

334
335 In the conserved N-terminal domains of FBS1 and FBS2 we found an overlapping LXLXL
336 sequence (Figure 1A), which is the most prominent form of an EAR motif found in many
337 different types of transcriptional regulators (Kagale and Rozwadowski, 2011; Shyu et al., 2012).
338 The EAR motif mediates interaction with the WD40 repeat-containing protein TOPLESS (TPL)
339 and TOPLESS RELATED (TPR) co-repressor proteins (Long, 2006; Pauwels et al., 2010;
340 Causier et al., 2012). We considered whether this LXLXL sequence in the N-terminal region of
341 FBS1 might: 1) function as a canonical EAR motif to interact with TOPLESS, and/or 2) if it
342 could be important for mediating interactions with FBIPs. However, substituting all three leucine
343 residues for alanine in FBS1 did not alter its interaction with FBIP1, and FBS1 did not interact
344 with TPL (both as bait or as prey) in our yeast two-hybrid system.

345
346 **FBS interactions with FBIP occur in the nucleus**
347

348 We next used bimolecular fluorescence complementation (BiFC) to test FBS interaction with
349 FBIP in plants and determine where the interaction occurs in a cell. FBS and FBIP family
350 proteins were expressed in *Nicotiana benthamiana* leaves as C-terminal fusions to either N-
351 terminal (nYFP) or C-terminal (cYFP) halves of yellow fluorescent protein (YFP). In multiple
352 independent experiments, YFP fluorescence was observed for pairings between FBS1 and FBIP1
353 and FBIP2 (Figure 4). This YFP signal co-localized with that of a co-infiltrated H2B-RFP
354 construct, which localizes exclusively in the nucleus (Wang et al., 2013), and shows that
355 interactions between FBS1 and FBIP proteins also occur in the nucleus. Similar experiments
356 found that FBS2 – FBS4 also interact with FBIP1 in the nucleus (Supplementary Figure S2). We
357 observed interactions for FBS3 and FBS4 with FBIP2 (Supplementary Figure S3), although we
358 note that these interactions were more variable in number of YFP positive nuclei across
359 independent replicates. We did not observe any interactions between FBS2 and FBIP2. All FBS
360 and FBIP fusion protein constructs were tested as pairs with empty nYFP or cYFP vectors, and
361 in all pairings we were unable to detect any fluorescent signal similar FBS/FBIP test pairs
362 (Supplementary Figure S4). These findings show that in plants FBS proteins participate in
363 family-wide interactions in the nucleus.

364
365 **FBS1 destabilizes FBIP1**
366

367 With interaction established between multiple FBS and FBIP protein pairs, we next asked if the
368 protein abundance relationship between FBS1 and FBIP1 is consistent with FBIP1 being a
369 ubiquitylation target of SCF^{FBS1}. If a protein is ubiquitylated by a particular SCF complex and
370 subsequently degraded by the 26S proteasome, then increasing abundance of the F-box
371 component typically increases in vivo targeting and decreases substrate abundance (dos Santos
372 Maraschin et al., 2009). We therefore tested the effects of varying FBS1 protein levels on FBIP1
373 abundance in our *N. benthamiana* expression system by co-infiltrating *Agrobacterium* harboring
374 these test constructs in different relative concentrations. Increasing the presence of FBS1 protein
375 resulted in a corresponding decrease in FBIP1 protein abundance by Western blot analysis
376 (Figure 5). In comparison, when FBS1 abundance was increased relative to co-infiltrated 14-3-3 λ
377 in an identical setup we did not observe any decrease in 14-3-3 λ abundance as the amount of
378 expressed FBS1 was increased (Supplementary Figure S5). This finding is congruous with
379 previous observations that FBS1 and 14-3-3 interactions are not consistent with targeting
380 (Sepulveda-Garcia and Rocha-Sosa, 2012). Therefore, because the abundance of FBIP1
381 decreases in an FBS1-dependent manner, we conclude that FBIPs are viable candidates for
382 SCF^{FBS1} ubiquitylation targets.

383

384 **Interaction between FBIP1 and NIGT1.1**

385

386 Interaction between FBS and FBIP protein families represents a newly recognized link between
387 an SCF complex with stress inducible components (ie. *FBS1* gene expression; 14-3-3 interaction)
388 and a potential targeting output. However, without knowing the precise biological function of
389 FBIP proteins we cannot know the consequences of FBS-FBIP interactions, nor can we strongly
390 connect FBS1 to an exact cellular pathway. Therefore, we examined protein interactions in the
391 SUBA4 database for FBIP1, with particular consideration for our findings that FBS and FBIP
392 interactions occur in the nucleus. One protein reported to interact with FBIP1 was Nitrate-
393 Inducible GARP-type Transcriptional Repressor 1.1 (NIGT1.1/HHO3; At1g25550). NIGT1.1 is
394 a DNA-binding transcriptional repressor and a central regulator of gene expression programs
395 that coordinate nitrate (NO₃⁻) and phosphate (PO₄³⁻) signaling and starvation responses in plants
396 (Kiba et al., 2018; Maeda et al., 2018; Ueda and Yanagisawa, 2019; Ueda et al., 2020a, 2020b).
397 We tested this predicted interaction between FBIP1 and NIGT1.1 in yeast two-hybrid assays and
398 observed growth on both less stringent (-TLH) and more stringent (-TLHA) conditions (Figure
399 6A). In BiFC, both FBIP1 and FBIP2 interacted with NIGT1.1 in the nucleus, as demonstrated
400 by co-localization with H2B-RFP (Figure 6B). These interactions link FBS proteins through
401 FBIP proteins to a DNA-binding transcriptional repressor, which suggests that at least one
402 function of FBS proteins is to directly regulate gene expression programs that relate to
403 environmental conditions (ie. nitrate and phosphate macronutrient availability).

404

405

406 **DISCUSSION**

407

408 Prior work with the FBS subfamily strongly alluded to its role in plant stress responses
409 (Maldonado-Calderon et al., 2012; Sepulveda-Garcia and Rocha-Sosa, 2012; Gonzalez et al.,
410 2017), but detailed understanding was limited by the unknown nature of ubiquitylation target(s)
411 and by possible redundancy within the *FBS* gene family. Here, we have identified a pair of
412 WD40 repeat-like superfamily proteins, FBIP1 and FBIP2, that both interact with FBS family

413 proteins. Family-wide interactions between FBS and FBIP proteins in plants indicate that
414 redundancy issues likely need to be circumvented before genetic approaches will yield full
415 insight into *FBS* gene function based on phenotype analysis. Nonetheless, FBIP proteins are
416 strong candidates for SCF^{FBS} ubiquitylation targeting. FBIP interaction with NIGT1.1, a key
417 regulator of nitrate responsive genes, directly links FBS proteins to nuclear and transcription
418 regulatory processes (Figure 7). Collectively, the FBS-FBIP-NIGT1.1 module is a new protein
419 interaction network in which to understand regulation of stress genes by an SCF-type E3 ligase
420 (Figure 7). Finally, FBIP and FBS interactions provide new context with which to investigate
421 FBX protein N-terminal events, and to further understand how this unique subfamily of FBX
422 proteins might couple N-terminal and C-terminal events to integrate cellular outputs to help
423 plants maintain resilience under environmental stress.

424

425 **The molecular function of FBIP proteins**

426

427 Our findings point to a direct role for FBS proteins in gene regulation, but knowing this with
428 certainty will require understanding the molecular function of FBIP proteins. Some plant
429 nuclear-localized WD40 repeat proteins have direct actions in transcription regulation (Causier et
430 al., 2012; Ke et al., 2015; Long and Schiefelbein, 2020) or chromatin modification (Li et al.,
431 2007; Zhu et al., 2008b; Mehdi et al., 2016), and knowledge of these roles should inform
432 hypotheses and future work. For example, TOPLESS (TPL) is a well-studied WD40 repeat-
433 containing co-repressor protein that interacts with multiple transcriptional complexes acting in
434 diverse pathways (ie. auxin, jasmonate, development) and recruits chromatin modifying enzymes
435 to repress gene expression (Krogan et al., 2012; Wang et al., 2013). TRANSPARENT TESTA
436 GLABRA 1 (TTG1), another WD40 repeat protein, serves as a scaffold and mediates different
437 combinations of bHLH and R2R3-type MYB transcription factors to regulate flavonoid
438 metabolism and various developmental processes (Lloyd et al., 2017; Long and Schiefelbein,
439 2020). Considering these established roles for WD40 repeat proteins in nuclear events, a few
440 possibilities seem readily apparent for FBIPs in the context of NIGT1.1-mediated transcription
441 regulation. First, FBIPs could recruit additional proteins that either enable or inhibit the
442 transcriptional repression activity of NIGT1.1, potentially by interfacing with chromatin
443 modifying enzymes, such as histone deacetylases (Wang et al., 2013). Second, as NIGT1.1 itself
444 belongs to a subfamily of four NIGT1 transcription factors that dimerize (Yanagisawa, 2013;
445 Ueda et al., 2020b), it is possible that FBIPs in some way mediate in vivo pairings and are
446 functionally analogous to TTG1. Furthermore, as there are 56 GARP-type transcriptional
447 repressors in *Arabidopsis* (Safi et al., 2017), it is possible that FBIP proteins could interact with
448 some of these other regulators to exert broader effects on gene regulation beyond nitrate- and
449 phosphate-dependent processes. We note that other GARP family transcription factors regulate
450 ABA- and JA-responsive genes (Merelo et al., 2013), and so past work showing that *FBS1*
451 impacts genes responsive to these two stress hormones is consistent with this notion (Gonzalez et
452 al., 2017). Future efforts will be aimed at understanding the full spectrum of interactions between
453 the two FBIP proteins and other GARP family transcription factors, with special focus on the
454 NIGT1 subfamily, as well as whether FBIPs interact with additional proteins that may assist in
455 gene regulation.

456

457 **FBIPs as candidate ubiquitylation targets**

458

459 A number of important questions surround the consequence of FBIP proteins as FBS interactors,
460 but hypotheses for immediate future work are equally apparent. Knowing that SCF complexes in
461 some unique contexts ubiquitylate targets via FBX protein N-terminal interactions (Lee et al.,
462 2018), and that FBS1 appears to destabilize FBIP1 (Figure 5), a leading hypothesis is that FBIP
463 proteins are bona fide ubiquitylation substrates for SCF^{FBS}. Rigorous assessment of in vivo
464 interaction dynamics between SCF^{FBS} complexes and FBIP proteins, and whether interaction
465 stimulates ubiquitylation-dependent degradation of FBIP proteins, will be critical lines of inquiry
466 in future work. Given the constitutive gene expression profile of *FBIP1* across publicly
467 accessible transcriptome data sets, it could be that FBIP proteins are components of a stress-
468 response system that is triggered at the post-translational level. An obvious following question,
469 then, is whether FBIP proteins are degraded in response to changing environmental conditions
470 and, if so, whether some factor (ie. post-translational modification) stimulates SCF^{FBS}
471 association with FBIP proteins under these conditions. The idea that additional in vivo factors or
472 modification mediates FBS/FBIP interaction is consistent with notion that we observed more
473 family-wide interactions in our in plant BiFC experiments compared to yeast two-hybrid.
474

475 With current understanding, however, we cannot completely exclude the possibility that FBIP
476 proteins are not targets, but instead serve an alternative function that enables (or inhibits) FBS
477 action. An idea with precedence is that FBIP proteins are accessories that recruit other proteins
478 as ubiquitylation targets. For example, in Arabidopsis, KAI2 and D14 interact with FBX protein
479 MAX2 in SCF^{MAX2} complex to mediate ubiquitylation of SMXL transcription factors (Wang et
480 al., 2020). In humans, Cks1 directly associates with the N-terminus of FBX protein Skp2 to
481 direct SCF^{Skp2} interaction with ubiquitylation target p27 in human cell cycle regulation (Spruck
482 et al., 2001; Skaar et al., 2013). A parallel, but intimately connected, line of questioning involves
483 identifying an FBS C-terminal region-interacting protein that we presume to exist. Knowing this
484 additional putative interactor may aid in addressing important aspects of FBIP function, and
485 future work can investigate the coordination of higher order complex assembly and/or possible
486 situations of dual targeting and co-occurring processes.
487

488 **FBS proteins are new tools with which to probe regulation of nitrate/phosphate starvation 489 responses**

490

491 Nitrate and phosphate are two indispensable macronutrients, but their abundances are highly
492 variable in most environments. The subfamily of four NIGT1 transcription factors directly
493 regulates hundreds of nitrate responsive genes by: 1) helping to elicit a quick-pulse response to
494 nitrate under some regulatory contexts (Ueda and Yanagisawa, 2019), or 2) control sustained
495 diminished expression in other regulatory contexts (Medici et al., 2015; Ueda and Yanagisawa,
496 2019). Nitrate uptake and assimilation by plants is intimately coordinated with that of phosphate,
497 and at least some regulatory events that accomplish this at the gene expression level occur
498 through NIGT1 activities (Ueda and Yanagisawa, 2019). Though functional relationships
499 between FBS, FBIP, and NIGT1.1 proteins are not yet known, recent work with NIGT1 proteins
500 and their regulation nitrate and phosphate responsive gene networks gives invaluable
501 experimental context for future work (Kiba et al., 2018; Maeda et al., 2018; Ueda et al., 2020a).
502 Coupling Arabidopsis genetic resources related to *FBS* and *FBIP* genes to those of *NIGT1.1* will
503 likely advance our understanding of how these factors work together, for example whether FBIP
504 proteins have a positive effect on NIGT1.1 (and other NIGT1 family proteins), to accomplish

505 regulation of nitrate-responsive transcriptional processes in various environmental contexts (ie.
506 cold or salt stress). Furthermore, as both *NIGT1* and *FBS1* are very rapidly induced by their
507 respective stress-inducing situations (Maldonado-Calderon et al., 2012; Sawaki et al., 2013;
508 Gonzalez et al., 2017), understanding how these factors work together may help further define
509 temporal priorities and resource management in nitrogen acquisition and other parts of stress
510 responses. Taken together, harnessing *FBS* and *FBIP* genes will present new opportunities by
511 which to understand how plants integrate and manage nitrate and phosphate stresses with other
512 stress conditions.

513
514 Different stress response pathways do not work in isolation (Rasmussen et al., 2013), but are
515 coordinated with one another to collectively contribute to comprehensive health of plants under
516 duress. However, much remains to be learned about the integration of different pathways. Given
517 its broad biotic and abiotic stress-triggered induction, as well as its stress hormone
518 responsiveness (Maldonado-Calderon et al., 2012; Gonzalez et al., 2017), *FBS1* may act in a
519 common cellular pathway or process that is more universally harnessed to aid compromised, or
520 otherwise challenged, plant cells. Further support for this notion comes from the fact that *FBS1*
521 interacts with multiple 14-3-3 proteins that work at least in both salt and cold stresses
522 (Sepulveda-Garcia and Rocha-Sosa, 2012; Catala et al., 2014; van Kleeff et al., 2014; Zhou et
523 al., 2014). The mechanistic connection delineated by an *FBS*/*FBIP*/*NIGT1* module may connect
524 a more globally induced environmental stress response to a nitrate uptake/assimilation program
525 mediated by *NIGT1* and co-acting proteins. In fact, nitrogen, in particular the nitrate and
526 ammonia forms, enhances plant performance in various forms of abiotic stress, as it is required
527 for *de novo* synthesis of various metabolites and proteins with protective properties (Zhang et al.,
528 2018; Rohilla and Yadav, 2019; Li et al., 2020). In seeming contrast, however, some abiotic
529 stress-responsive transcriptional networks naturally limit expression of genes central to nitrogen
530 uptake and assimilation (Goel and Singh, 2015). These observations underscore the notion that
531 there is still much to learn about the complexities of these gene regulatory networks and
532 physiological processes acting in broader stress contexts. This work, including the subsequent
533 hypotheses it generates, provides a new mechanistic framework in which to assess how an
534 atypical SCF complex may coordinate cellular stress pathways, including those acting in nitrate
535 and phosphate uptake and assimilation, through transcription regulation events.

536

537

538 **FUNDING**

539

540 This work was supported by grants from the M.J. Murdock Charitable Trust (NS-2016262 and
541 20141205:MNL:11/20/14) for materials and student summer research stipends, and funds from
542 University Enrichment Committee (UEC) at the University of Puget Sound for materials and
543 student summer research stipends.

544

545

546 **AUTHOR CONTRIBUTIONS**

547

548 ESG, ECF, EVP, AAB, LEO, AAF, AJR, and BT conducted the experiments. All authors
549 designed the experiments, analyzed the data, and approved the final version of the manuscript.
550 BT wrote the manuscript.

551

552

553 ACKNOWLEDGEMENTS

554

555 We thank David Somers (The Ohio State University) for the H2B-RFP construct, Frank Harmon
556 (University of California at Berkeley / USDA Plant Gene Expression Center) for the yeast two-
557 hybrid vectors, Faride Unda (University of British Columbia) for the BiFC vectors, and Ruirui
558 Huang and Vivian Irish (Yale University) for the yeast two-hybrid TOPLESS constructs. We
559 also thank Marisa Weiss for her help with cloning *NIGT1.1* and Andreas Madlung (University of
560 Puget Sound) for critical reading of the manuscript and other helpful discussions. Finally, we
561 would like to thank Michal Morrison-Kerr (University of Puget Sound) for her indispensable
562 help in supporting Puget Sound undergraduate research students.

563

564

565 REFERENCES

566

567 Arabidopsis Interactome Mapping Consortium, Dreze, M., Carvunis, A.-R., Charlotteaux, B.,
568 Galli, M., Pevzner, S. J., et al. (2011). Evidence for Network Evolution in an Arabidopsis
569 Interactome Map. *Science* 333, 601–607. doi:10.1126/science.1203877.

570 Calderon Villalobos, L. I., Lee, S., De Oliveira, C., Ivetac, A., Brandt, W., Armitage, L., et al.
571 (2012). A combinatorial TIR1/AFB-Aux/IAA co-receptor system for differential sensing
572 of auxin. *Nat Chem Biol* 8, 477–85. doi:10.1038/nchembio.926.

573 Catala, R., Lopez-Cobollo, R., Mar Castellano, M., Angosto, T., Alonso, J. M., Ecker, J. R., et al.
574 (2014). The Arabidopsis 14-3-3 protein RARE COLD INDUCIBLE 1A links low-
575 temperature response and ethylene biosynthesis to regulate freezing tolerance and cold
576 acclimation. *Plant Cell* 26, 3326–42. doi:10.1105/tpc.114.127605.

577 Causier, B., Ashworth, M., Guo, W., and Davies, B. (2012). The TOPLESS Interactome: A
578 Framework for Gene Repression in Arabidopsis. *PLANT Physiol.* 158, 423–438.
579 doi:10.1104/pp.111.186999.

580 dos Santos Maraschin, F., Memelink, J., and Offringa, R. (2009). Auxin-induced, SCF^{TIR1} -
581 mediated poly-ubiquitination marks AUX/IAA proteins for degradation. *Plant J.* 59,
582 100–109. doi:10.1111/j.1365-313X.2009.03854.x.

583 Gagne, J. M., Downes, B. P., Shiu, S. H., Durski, A. M., and Vierstra, R. D. (2002). The F-box
584 subunit of the SCF E3 complex is encoded by a diverse superfamily of genes in
585 Arabidopsis. *Proc Natl Acad Sci U A* 99, 11519–24. doi:10.1073/pnas.162339999.

586 Goda, H., Sasaki, E., Akiyama, K., Maruyama-Nakashita, A., Nakabayashi, K., Li, W., et al.
587 (2008). The AtGenExpress hormone and chemical treatment data set: experimental
588 design, data evaluation, model data analysis and data access. *Plant J.* 55, 526–542.
589 doi:10.1111/j.1365-313X.2008.03510.x.

590 Goel, P., and Singh, A. K. (2015). Abiotic Stresses Downregulate Key Genes Involved in
591 Nitrogen Uptake and Assimilation in *Brassica juncea* L. *PLOS ONE* 10, e0143645.
592 doi:10.1371/journal.pone.0143645.

593 Gonzalez, L. E., Keller, K., Chan, K. X., Gessel, M. M., and Thines, B. C. (2017). Transcriptome
594 analysis uncovers *Arabidopsis* F-BOX STRESS INDUCED 1 as a regulator of jasmonic
595 acid and abscisic acid stress gene expression. *BMC Genomics* 18. doi:10.1186/s12864-
596 017-3864-6.

597 Hooper, C. M., Castleden, I. R., Tanz, S. K., Aryamanesh, N., and Millar, A. H. (2017). SUBA4:
598 the interactive data analysis centre for *Arabidopsis* subcellular protein locations. *Nucleic
599 Acids Res.* 45, D1064–D1074. doi:10.1093/nar/gkw1041.

600 Hua, Z., and Vierstra, R. D. (2011). The cullin-RING ubiquitin-protein ligases. *Annu Rev Plant
601 Biol* 62, 299–334. doi:10.1146/annurev-arplant-042809-112256.

602 Jain, B. P., and Pandey, S. (2018). WD40 Repeat Proteins: Signalling Scaffold with Diverse
603 Functions. *Protein J.* 37, 391–406. doi:10.1007/s10930-018-9785-7.

604 Jin, J. (2004). Systematic analysis and nomenclature of mammalian F-box proteins. *Genes Dev.*
605 18, 2573–2580. doi:10.1101/gad.1255304.

606 Kagale, S., and Rozwadowski, K. (2011). EAR motif-mediated transcriptional repression in
607 plants: An underlying mechanism for epigenetic regulation of gene expression.
608 *Epigenetics* 6, 141–146. doi:10.4161/epi.6.2.13627.

609 Ke, J., Ma, H., Gu, X., Thelen, A., Brunzelle, J. S., Li, J., et al. (2015). Structural basis for
610 recognition of diverse transcriptional repressors by the TOPLESS family of corepressors.
611 *Sci. Adv.* 1, e1500107. doi:10.1126/sciadv.1500107.

612 Kiba, T., Inaba, J., Kudo, T., Ueda, N., Konishi, M., Mitsuda, N., et al. (2018). Repression of
613 Nitrogen Starvation Responses by Members of the *Arabidopsis* GARP-Type
614 Transcription Factor NIGT1/HRS1 Subfamily. *Plant Cell* 30, 925–945.
615 doi:10.1105/tpc.17.00810.

616 Kilian, J., Whitehead, D., Horak, J., Wanke, D., Weinl, S., Batistic, O., et al. (2007). The
617 AtGenExpress global stress expression data set: protocols, evaluation and model data
618 analysis of UV-B light, drought and cold stress responses. *Plant J* 50, 347–63.
619 doi:10.1111/j.1365-313X.2007.03052.x.

620 Kim, W. Y., Fujiwara, S., Suh, S. S., Kim, J., Kim, Y., Han, L., et al. (2007). ZEITLUPE is a
621 circadian photoreceptor stabilized by GIGANTEA in blue light. *Nature* 449, 356–60.
622 doi:10.1038/nature06132.

623 Kirk, R., Laman, H., Knowles, P. P., Murray-Rust, J., Lomonosov, M., Meziane, E. K., et al.
624 (2008). Structure of a Conserved Dimerization Domain within the F-box Protein Fbxo7
625 and the PI31 Proteasome Inhibitor. *J. Biol. Chem.* 283, 22325–22335.
626 doi:10.1074/jbc.M709900200.

627 Krogan, N. T., Hogan, K., and Long, J. A. (2012). APETALA2 negatively regulates multiple
628 floral organ identity genes in *Arabidopsis* by recruiting the co-repressor TOPLESS and
629 the histone deacetylase HDA19. *Development* 139, 4180–4190. doi:10.1242/dev.085407.

630 Kuroda, H., Yanagawa, Y., Takahashi, N., Horii, Y., and Matsui, M. (2012). A comprehensive
631 analysis of interaction and localization of *Arabidopsis* SKP1-like (ASK) and F-box
632 (FBX) proteins. *PLoS One* 7, e50009. doi:10.1371/journal.pone.0050009.

633 Lee, C.-M., Feke, A., Li, M.-W., Adamchek, C., Webb, K., Pruneda-Paz, J., et al. (2018).
634 Decoys Untangle Complicated Redundancy and Reveal Targets of Circadian Clock F-
635 Box Proteins. *Plant Physiol.* 177, 1170–1186. doi:10.1104/pp.18.00331.

636 Li, H., He, Z., Lu, G., Lee, S. C., Alonso, J., Ecker, J. R., et al. (2007). A WD40 Domain
637 Cyclophilin Interacts with Histone H3 and Functions in Gene Repression and
638 Organogenesis in *Arabidopsis*. *Plant Cell* 19, 2403–2416. doi:10.1105/tpc.107.053579.

639 Li, S., Zhou, L., Addo-Danso, S. D., Ding, G., Sun, M., Wu, S., et al. (2020). Nitrogen supply
640 enhances the physiological resistance of Chinese fir plantlets under polyethylene glycol
641 (PEG)-induced drought stress. *Sci. Rep.* 10, 7509. doi:10.1038/s41598-020-64161-7.

642 Lloyd, A., Brockman, A., Aguirre, L., Campbell, A., Bean, A., Cantero, A., et al. (2017).
643 Advances in the MYB–bHLH–WD Repeat (MBW) Pigment Regulatory Model: Addition
644 of a WRKY Factor and Co-option of an Anthocyanin MYB for Betalain Regulation.
645 *Plant Cell Physiol.* 58, 1431–1441. doi:10.1093/pcp/pcx075.

646 Long, J. A. (2006). TOPLESS Regulates Apical Embryonic Fate in *Arabidopsis*. *Science* 312,
647 1520–1523. doi:10.1126/science.1123841.

648 Long, Y., and Schiefelbein, J. (2020). Novel TTG1 Mutants Modify Root-Hair Pattern
649 Formation in *Arabidopsis*. *Front. Plant Sci.* 11, 383. doi:10.3389/fpls.2020.00383.

650 Ma, J., An, K., Zhou, J.-B., Wu, N.-S., Wang, Y., Ye, Z.-Q., et al. (2019). WDSPdb: an updated
651 resource for WD40 proteins. *Bioinformatics* 35, 4824–4826.
652 doi:10.1093/bioinformatics/btz460.

653 Maeda, Y., Konishi, M., Kiba, T., Sakuraba, Y., Sawaki, N., Kurai, T., et al. (2018). A NIGT1-
654 centred transcriptional cascade regulates nitrate signalling and incorporates phosphorus
655 starvation signals in *Arabidopsis*. *Nat. Commun.* 9, 1376. doi:10.1038/s41467-018-
656 03832-6.

657 Maldonado-Calderon, M. T., Sepulveda-Garcia, E., and Rocha-Sosa, M. (2012). Characterization
658 of novel F-box proteins in plants induced by biotic and abiotic stress. *Plant Sci* 185–186,
659 208–17. doi:10.1016/j.plantsci.2011.10.013.

660 Más, P., Kim, W.-Y., Somers, D. E., and Kay, S. A. (2003). Targeted degradation of TOC1 by
661 ZTL modulates circadian function in *Arabidopsis thaliana*. *Nature* 426, 567–570.
662 doi:10.1038/nature02163.

663 Matsumoto, A., Tateishi, Y., Onoyama, I., Okita, Y., Nakayama, K., and Nakayama, K. I.
664 (2011). Fbxw7 β resides in the endoplasmic reticulum membrane and protects cells from
665 oxidative stress. *Cancer Sci.* 102, 749–755. doi:10.1111/j.1349-7006.2011.01851.x.

666 Medici, A., Marshall-Colon, A., Ronzier, E., Szponarski, W., Wang, R., Gojon, A., et al. (2015).
667 AtNIGT1/HRS1 integrates nitrate and phosphate signals at the Arabidopsis root tip. *Nat.*
668 *Commun.* 6, 6274. doi:10.1038/ncomms7274.

669 Mehdi, S., Derkacheva, M., Ramström, M., Kralemann, L., Bergquist, J., and Hennig, L. (2016).
670 The WD40 Domain Protein MSI1 Functions in a Histone Deacetylase Complex to Fine-
671 Tune Abscisic Acid Signaling. *Plant Cell* 28, 42–54. doi:10.1105/tpc.15.00763.

672 Merelo, P., Xie, Y., Brand, L., Ott, F., Weigel, D., Bowman, J. L., et al. (2013). Genome-Wide
673 Identification of KANADI1 Target Genes. *PLoS ONE* 8, e77341.
674 doi:10.1371/journal.pone.0077341.

675 Nakagawa, T., Kurose, T., Hino, T., Tanaka, K., Kawamukai, M., Niwa, Y., et al. (2007).
676 Development of series of gateway binary vectors, pGWBs, for realizing efficient
677 construction of fusion genes for plant transformation. *J. Biosci. Bioeng.* 104, 34–41.

678 Nelson, D. E., Randle, S. J., and Laman, H. (2013). Beyond ubiquitination: the atypical functions
679 of Fbxo7 and other F-box proteins. *Open Biol.* 3, 130131. doi:10.1098/rsob.130131.

680 Pauwels, L., Barbero, G. F., Geerinck, J., Tillemen, S., Grunewald, W., Pérez, A. C., et al.
681 (2010). NINJA connects the co-repressor TOPLESS to jasmonate signalling. *Nature* 464,
682 788–791. doi:10.1038/nature08854.

683 Rasmussen, S., Barah, P., Suarez-Rodriguez, M. C., Bressendorff, S., Friis, P., Costantino, P., et
684 al. (2013). Transcriptome Responses to Combinations of Stresses in Arabidopsis. *Plant*
685 *Physiol.* 161, 1783–1794. doi:10.1104/pp.112.210773.

686 Rohilla, P., and Yadav, J. P. (2019). Acute salt stress differentially modulates nitrate reductase
687 expression in contrasting salt responsive rice cultivars. *Protoplasma* 256, 1267–1278.
688 doi:10.1007/s00709-019-01378-y.

689 Safi, A., Medici, A., Szponarski, W., Ruffel, S., Lacombe, B., and Krouk, G. (2017). The world
690 according to GARP transcription factors. *Curr. Opin. Plant Biol.* 39, 159–167.
691 doi:10.1016/j.pbi.2017.07.006.

692 Sawa, M., Nusinow, D. A., Kay, S. A., and Imaizumi, T. (2007). FKF1 and GIGANTEA
693 Complex Formation Is Required for Day-Length Measurement in Arabidopsis. *Science*
694 318, 261–265. doi:10.1126/science.1146994.

695 Sawaki, N., Tsujimoto, R., Shigyo, M., Konishi, M., Toki, S., Fujiwara, T., et al. (2013). A
696 Nitrate-Inducible GARP Family Gene Encodes an Auto-Repressible Transcriptional
697 Repressor in Rice. *Plant Cell Physiol.* 54, 506–517. doi:10.1093/pcp/pct007.

698 Schmid, M., Davison, T. S., Henz, S. R., Pape, U. J., Demar, M., Vingron, M., et al. (2005). A
699 gene expression map of *Arabidopsis thaliana* development. *Nat Genet* 37, 501–6.
700 doi:10.1038/ng1543.

701 Sepulveda-Garcia, E., and Rocha-Sosa, M. (2012). The *Arabidopsis* F-box protein AtFBS1
702 interacts with 14-3-3 proteins. *Plant Sci* 195, 36–47. doi:10.1016/j.plantsci.2012.06.009.

703 Sheard, L. B., Tan, X., Mao, H., Withers, J., Ben-Nissan, G., Hinds, T. R., et al. (2010).
704 Jasmonate perception by inositol-phosphate-potentiated COI1-JAZ co-receptor. *Nature*
705 468, 400–5. doi:10.1038/nature09430.

706 Shyu, C., Figueroa, P., DePew, C. L., Cooke, T. F., Sheard, L. B., Moreno, J. E., et al. (2012).
707 JAZ8 Lacks a Canonical Degron and Has an EAR Motif That Mediates Transcriptional
708 Repression of Jasmonate Responses in *Arabidopsis*. *PLANT CELL ONLINE* 24, 536–550.
709 doi:10.1105/tpc.111.093005.

710 Skaar, J. R., Pagan, J. K., and Pagano, M. (2013). Mechanisms and function of substrate
711 recruitment by F-box proteins. *Nat. Rev. Mol. Cell Biol.* 14, 369–381.
712 doi:10.1038/nrm3582.

713 Song, Y. H., Estrada, D. A., Johnson, R. S., Kim, S. K., Lee, S. Y., MacCoss, M. J., et al. (2014).
714 Distinct roles of FKF1, GIGANTEA, and ZEITLUPE proteins in the regulation of
715 CONSTANS stability in *Arabidopsis* photoperiodic flowering. *Proc Natl Acad Sci U A*
716 111, 17672–7. doi:10.1073/pnas.1415375111.

717 Spruck, C., Strohmaier, H., Watson, M., Smith, A. P. L., Ryan, A., Krek, W., et al. A CDK-
718 Independent Function of Mammalian Cks1: Targeting of SCFSkp2 to the CDK Inhibitor
719 p27kip. *Mol. Cell*, 12.

720 Ueda, Y., Kiba, T., and Yanagisawa, S. (2020a). Nitrate-inducible NIGT1 proteins modulate
721 phosphate uptake and starvation signalling via transcriptional regulation of *SPX* genes.
722 *Plant J.* 102, 448–466. doi:10.1111/tpj.14637.

723 Ueda, Y., Nosaki, S., Sakuraba, Y., Miyakawa, T., Kiba, T., Tanokura, M., et al. (2020b).
724 NIGT1 family proteins exhibit dual mode DNA recognition to regulate nutrient response-
725 associated genes in *Arabidopsis*. *PLOS Genet.* 16, e1009197.
726 doi:10.1371/journal.pgen.1009197.

727 Ueda, Y., and Yanagisawa, S. (2019). Perception, transduction, and integration of nitrogen and
728 phosphorus nutritional signals in the transcriptional regulatory network in plants. *J. Exp.*
729 *Bot.* 70, 3709–3717. doi:10.1093/jxb/erz148.

730 van Kleeff, P. J., Jaspert, N., Li, K. W., Rauch, S., Oecking, C., and de Boer, A. H. (2014).
731 Higher order *Arabidopsis* 14-3-3 mutants show 14-3-3 involvement in primary root
732 growth both under control and abiotic stress conditions. *J Exp Bot* 65, 5877–88.
733 doi:10.1093/jxb/eru338.

734 Wang, L., Kim, J., and Somers, D. E. (2013). Transcriptional corepressor TOPLESS complexes
735 with pseudoresponse regulator proteins and histone deacetylases to regulate circadian
736 transcription. *Proc. Natl. Acad. Sci.* 110, 761–766. doi:10.1073/pnas.1215010110.

737 Wang, L., Xu, Q., Yu, H., Ma, H., Li, X., Yang, J., et al. (2020). Strigolactone and Karrkin
738 Signaling Pathways Elicit Ubiquitination and Proteolysis of SMXL2 to Regulate
739 Hypocotyl Elongation in *Arabidopsis thaliana*. *Plant Cell*, tpc.00140.2020.
740 doi:10.1105/tpc.20.00140.

741 Wang, Z., Liu, P., Inuzuka, H., and Wei, W. (2014). Roles of F-box proteins in cancer. *Nat. Rev. Cancer* 14, 233–247. doi:10.1038/nrc3700.

743 Yanagisawa, S. (2013). Characterization of a nitrate-inducible transcriptional repressor NIGT1
744 provides new insights into DNA recognition by the GARP family proteins. *Plant Signal. Behav.* 8, e24447. doi:10.4161/psb.24447.

746 Yasuhara, M. (2004). Identification of ASK and clock-associated proteins as molecular partners
747 of LKP2 (LOV kelch protein 2) in *Arabidopsis*. *J. Exp. Bot.* 55, 2015–2027.
748 doi:10.1093/jxb/erh226.

749 Zhang, G.-B., Meng, S., and Gong, J.-M. (2018). The Expected and Unexpected Roles of Nitrate
750 Transporters in Plant Abiotic Stress Resistance and Their Regulation. *Int. J. Mol. Sci.* 19,
751 3535. doi:10.3390/ijms19113535.

752 Zhou, H., Lin, H., Chen, S., Becker, K., Yang, Y., Zhao, J., et al. (2014). Inhibition of the
753 *Arabidopsis* salt overly sensitive pathway by 14-3-3 proteins. *Plant Cell* 26, 1166–82.
754 doi:10.1105/tpc.113.117069.

755 Zhu, D., Maier, A., Lee, J.-H., Laubinger, S., Saijo, Y., Wang, H., et al. (2008a). Biochemical
756 Characterization of *Arabidopsis* Complexes Containing CONSTITUTIVELY
757 PHOTOMORPHOGENIC1 and SUPPRESSOR OF PHYA Proteins in Light Control of
758 Plant Development. *Plant Cell* 20, 2307–2323. doi:10.1105/tpc.107.056580.

759 Zhu, J., Jeong, J. C., Zhu, Y., Sokolchik, I., Miyazaki, S., Zhu, J.-K., et al. (2008b). Involvement
760 of *Arabidopsis* HOS15 in histone deacetylation and cold tolerance. *Proc. Natl. Acad. Sci.*
761 105, 4945–4950. doi:10.1073/pnas.0801029105.

762 Zoltowski, B. D., and Imaizumi, T. (2014). “Structure and Function of the ZTL/FKF1/LKP2
763 Group Proteins in *Arabidopsis*,” in *The Enzymes* (Elsevier), 213–239. doi:10.1016/B978-
764 0-12-801922-1.00009-9.

765

766 **FIGURE LEGENDS**

767

768 **Figure 1. The F-BOX STRESS INDUCED (FBS) protein family.** (A) Full-length protein
769 sequence alignment of the four *Arabidopsis* FBS family members (FBS1 – FBS4) created with
770 T-COFFEE sequence alignment program. Asterisks are fully conserved residues, colons are
771 strongly conserved residue properties, and periods are weakly conserved residue properties. (B)

772 FBS family interactions with ASK1 in yeast two-hybrid assays. Diploid yeast strains with
773 indicated test constructs as bait (DBD) and prey (AD) were grown in liquid culture, diluted
774 ($OD_{600} = 10^0, 10^{-1}, 10^{-2}, 10^{-3}$), and spotted on SD medium minus Trp/Leu (-TL), minus
775 Trp/Leu/His (-TLH), and minus Trp/Leu/His/Ade (-TLHA).

776
777 **Figure 2. FBS INTERACTING PROTEIN (FBIP) sequence features.** Full-length protein
778 sequence alignment of the two *Arabidopsis* FBIP family members created with T-COFFEE
779 sequence alignment program. Blue indicates locations of seven WD40-like repeat sequences
780 predicted by the WD40-repeat protein Structure Predictor version 2.0 (WDSRdb 2.0). Asterisks
781 are fully conserved residues, colons are strongly conserved residue properties, and periods are
782 weakly conserved residue properties.

783
784 **Figure 3. Yeast two-hybrid (Y2H) interactions between FBS1 and FBIP proteins. (A)** Full-
785 length FBS1 interactions with full-length FBIP1 and FBIP2. Diploid yeast strains with indicated
786 test constructs as bait (DBD) and prey (AD) were grown in liquid culture, diluted ($OD_{600} = 10^0,$
787 $10^{-1}, 10^{-2}, 10^{-3}$), and spotted on SD medium minus Trp/Leu (-TL), minus Trp/Leu/His (-TLH),
788 and minus Trp/Leu/His/Ade (-TLHA). **(B)** Truncated FBS1 bait (DBD) construct interaction
789 with full length FBIP1 prey (AD). Amino acid deletions are indicated on left.

790
791 **Figure 4. Bimolecular fluorescence complementation (BiFC) interactions between FBS1**
792 **and FBIP proteins.** Laser-scanning confocal microscopy of *N. benthamiana* epidermal cells
793 expressing N-terminal nYFP- or cYFP-tagged FBS1 and FBIP proteins. FBS1 interactions with
794 FBIP1 (top row) or FBIP2 (bottom row) are visualized on BiFC yellow channel (YFP, left
795 column). A co-expressed H2B-RFP (as nuclear marker) is visualized on red channel (RFP,
796 middle column) and YFP/RFP images are overlaid (Merge, right column). Arrow indicates
797 selected nuclei in expanded inset image. Scale bar = 100 μ m

798
799 **Figure 5. FBS1 influence on FBIP1 protein abundance in plants.** *N. benthamiana* leaves were
800 infiltrated with *Agrobacterium* (C58C1) strains to express tagged proteins. *Agrobacterium* mixes
801 contained varying cell densities of strains harboring expression constructs (myc-FBS1 and/or
802 FBIP1-HA), a suppressor protein (p19), or untransformed cells. Total protein was isolated from
803 leaves three days after infiltration, separated by SDS-PAGE, transferred, and probed with
804 antibodies against myc (top row, FBS1) or HA (second row, FBIP1). Bottom two rows show
805 Ponceau S staining of the major subunit of Rubisco from the same two blots as a loading control.

806
807 **Figure 6. FBIP interactions with transcriptional repressor NIGT1.1. (A)** Interaction between
808 full-length FBIP1 and full-length NIGT1.1 in yeast two-hybrid assays. Diploid yeast strains with
809 indicated test constructs as bait (DBD) and prey (AD) were grown in liquid culture, diluted
810 ($OD_{600} = 10^0, 10^{-1}, 10^{-2}, 10^{-3}$), and spotted on SD medium minus Trp/Leu (-TL), minus
811 Trp/Leu/His (-TLH), and minus Trp/Leu/His/Ade (-TLHA). **(B)** Laser-scanning confocal
812 microscopy of *N. benthamiana* epidermal cells expressing N-terminal nYFP- or cYFP-tagged
813 FBIP and NIGT1.1 proteins. NIGT1.1 interactions with FBIP1 (top row) or FBIP2 (bottom row)
814 are visualized on BiFC yellow channel (YFP, left column). A co-expressed H2B-RFP (as
815 nuclear marker) is visualized on red channel (RFP, middle column) and YFP/RFP images are
816 overlaid (Merge, right column). Arrow indicates selected nuclei in expanded inset image. Scale
817 bar = 100 μ m

818

819 **Figure 7. Integration of FBS proteins in a plant stress network.**

820

821 (A) Stress regulates FBS function through *FBS1* gene induction and possible control imposed by
822 14-3-3 proteins, which are negative regulators of abiotic stress responses. (B) SCF^{FBS} complexes
823 ubiquitylate (Ub) FBIP through FBS N-terminal (NT) interactions and also target an unknown
824 protein by FBS C-terminal (CT) interactions. Targets are degraded by the 26S proteasome
825 leading to cellular changes under stress conditions. (C) NIGT1.1 dimerizes with other NIGT1
826 transcription factors and binds promoter regions of nitrate responsive genes. FBIP interacts
827 NIGT1.1, and possibly with other NIGT1 and GARP-type transcription factors to influence their
828 activity. Action by FBIP might influence in vivo dimerization, recruit additional gene regulation
829 factors, alter DNA binding, or carry out some other function.

830

831

832

833

834

835

836

837

838

839

840

841

842

843

844

845

846

847

848

849

850

851

852

853

854

855

856

857

858

859

860

861

862

863

864 FIGURES

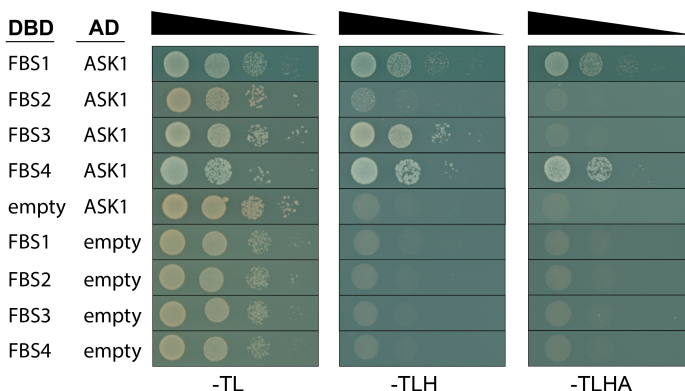
865

Figure 1

867

(A)

(B)



868

869

870

871

872

873

874

875

875

876

877

878

879

880

881

882 **Figure 2**
883

FBIP1 -MEGRRITASPRPCSG-RRIVAKKRSRPDGFBVNSVKKLQRREISSRKDRA
FBIP2 MMEGRRIIANPRPCSGSRRVIACKRSRPDGFBVNSVKKLQRREISSRMDRA
***** *.****** * :*****:*****:*****:*****:*****:*****:*****

FBIP1 FSISTAQERFRNMRLVEQYDTHDPKGHCLVALPFLMKRTKVIEIVAARDI
FBIP2 FSISTAQERFRNMRLVEQYDTHDPKGYCLVSLPNLLKRSKVIEIVAARDI
*****:*****:*****:*****:*****:*****:*****:*****

FBIP1 VFALAHSGVCAAFSRESNKRICFLNVSPDEVIRSLFYNKNNDSLITVSVY
FBIP2 VFALTLSGVCAFSSRETNKKVCFLNVSPDEVIRSLFYNKNNDSLITVSVY
*****:*****:*****:*****:*****:*****:*****

FBIP1 ASDNFSSLKCRSTRIEYILRGQPDAGFALFESESLKWPGBEFDDVNGKV
FBIP2 ASDNYSSLKCRSTRIEYILRGQADAGFPLFESESLKWPGBEFDDVNGKV
*****:*****:*****:*****:*****:*****

FBIP1 LTYSAQDSVYKVFDLKNYTMLYSISDKNVQEIKISPGIMLLIFKRAASHV
FBIP2 LTYSAQDSVYKVFDLKNYALLYSISDKNVQEIKISPGIMLLIFKRAASHV
*****:*****:*****:*****:*****

FBIP1 PLKILSIEDGTVLKSFnHLLHRNKKVDFIEQFNEKLLVKQENENLQILDV
FBIP2 PLKILSIEDGTLKSFHLLHRNKKVDFIEQFNEKLLVKQENENLQILDV
*****:*****:*****:*****

FBIP1 RNAELMEVSRAEFMTPSAFIFLYENQLFLTFRNRNVSVWNFRGELVTSFE
FBIP2 RNAELIEVSRTDFMTPSAFIFLYENQLFLTFRNRNVSVWNFRGELVTSFE
*****:*****:*****:*****

FBIP1 DHLLWHPDCNTNNIYITSQDLIISYCKADTEDQWIEGNAGSINISNILT
FBIP2 DHLLWHPDCNTNNIYITSQDLIISYCKADTEDQWIEGNAGSINISNILT
*****:*****:*****:*****

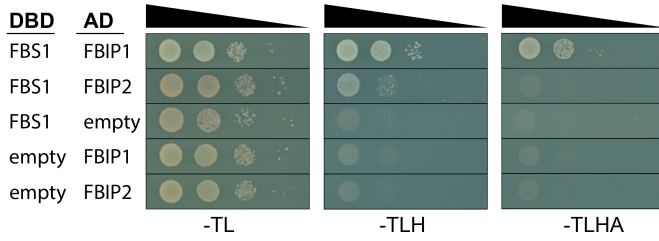
FBIP1 GKCLAKITPSSGPPKDDDESSSNCMGKNSQRRNAVAEALEDITALFYDE
FBIP2 GKCLAKIKANGPPKEEDCSSDL-G-NSSRRRSAVAEEALEDITALFYDE
*****:...*****:*****:*****:*****:*****:*****:*****

FBIP1 ERNEIYTGNRHGLVHVWSN
FBIP2 ERNEIYTGNRHGLLHVWSN
*****:*****:*****:*****

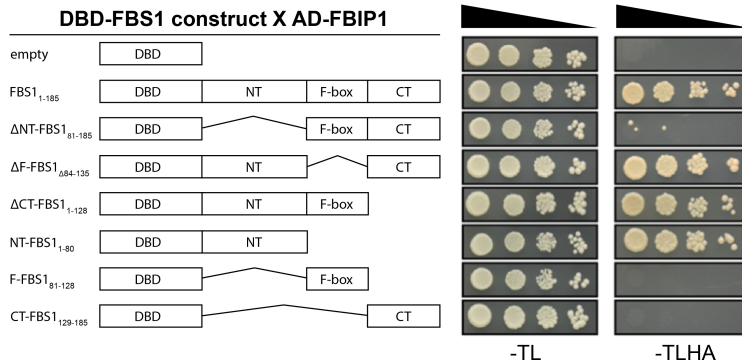
884
885
886
887
888
889
890
891
892
893
894
895
896
897
898
899
900
901
902

903 **Figure 3**
904

(A)

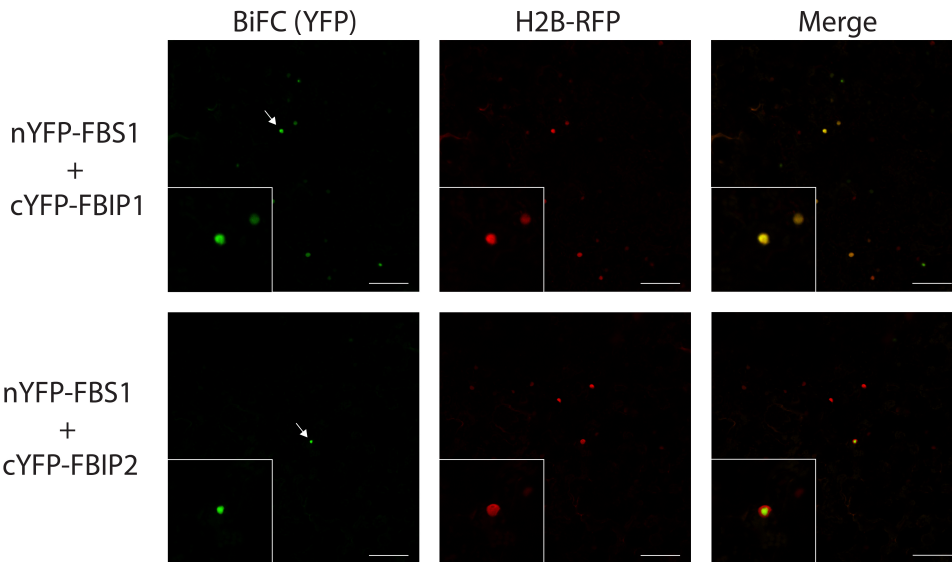


(B)



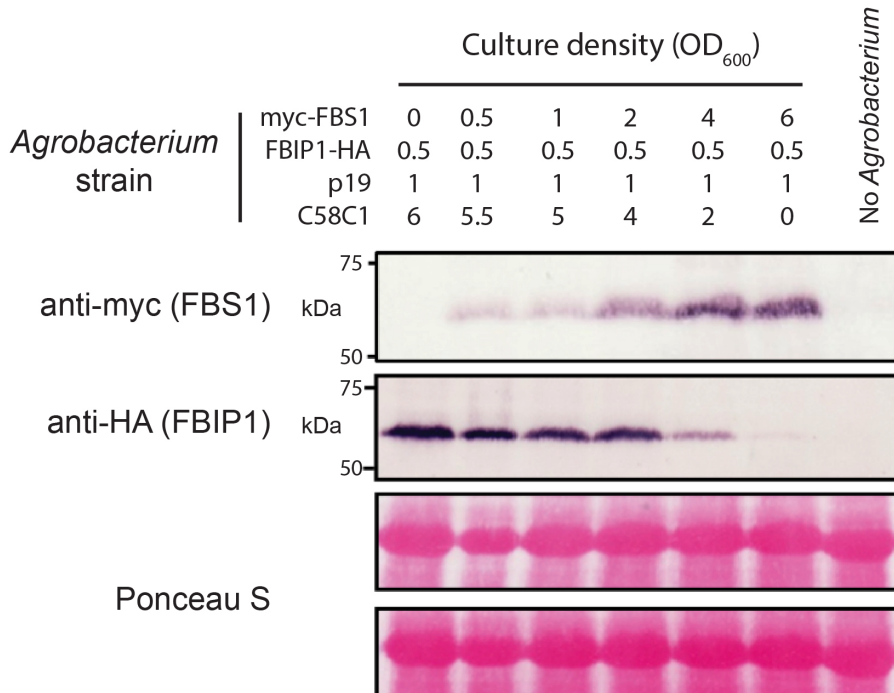
905
906
907
908
909
910
911
912
913
914
915
916
917
918
919
920
921
922
923
924
925
926
927

928 **Figure 4**
929



930
931
932
933
934
935
936
937
938
939
940
941
942
943
944
945
946
947
948
949
950
951
952
953
954
955
956
957
958
959

960 **Figure 5**
961

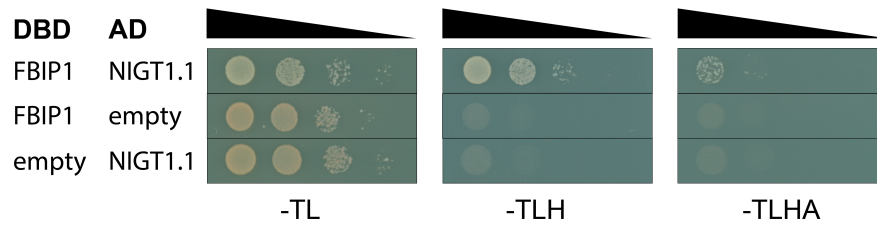


962
963
964
965
966
967
968
969
970
971
972
973
974
975
976
977
978
979
980
981
982
983
984
985
986
987

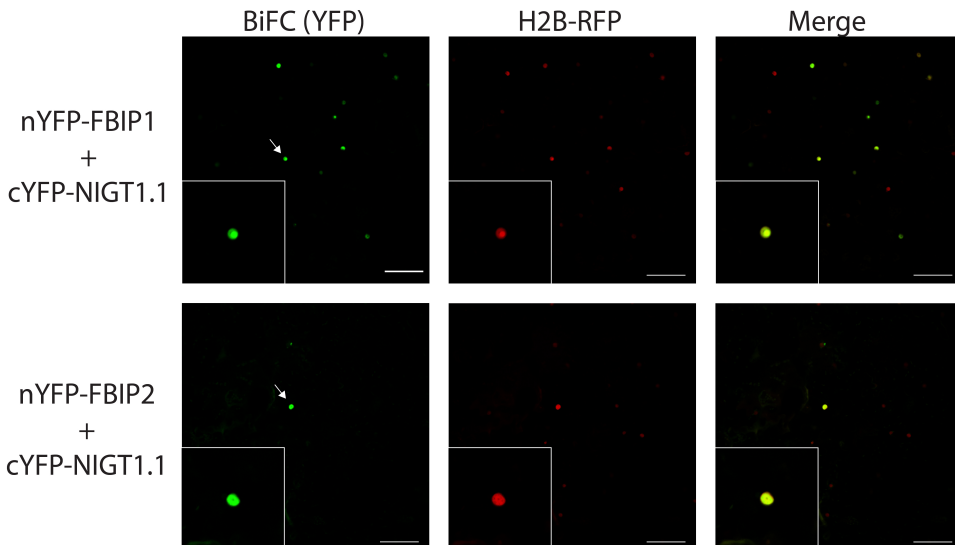
988 **Figure 6**

989

(A)



(B)



990

991

992

993

994

995

996

997

998

999

1000

1001

1002

1003

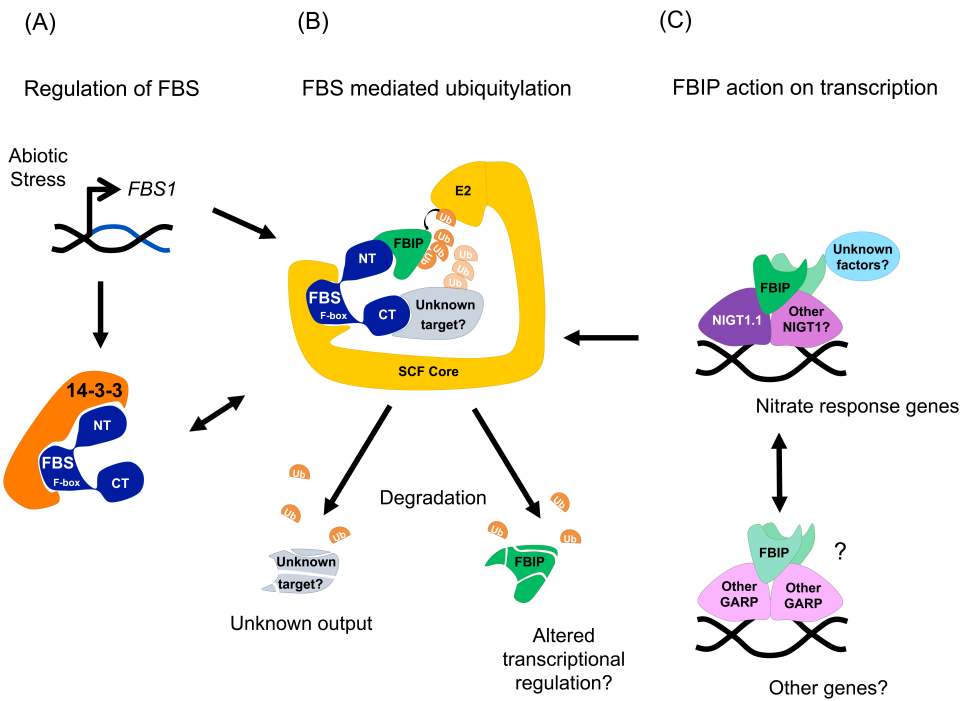
1004

1005

1006

1007 **Figure 7**

1008



1009

1010

1011

1012

1013

1014

1015

1016

1017

1018

1019

1020

1021

1022

1023

1024

1025

1026